

Inhibition of Aluminium Corrosion Using *Carica papaya* Leaves Extract in Sulphuric Acid

Baruku Kasuga^{1*}, Eugene Park¹, Revocatus L. Machunda²

¹Department of Materials and Energy Science & Engineering, Nelson Mandela African Institution of Science and Technology, Arusha, Tanzania

²Department of Water and Environmental Science and Engineering, Nelson Mandela African Institution of Science and Technology, Arusha, Tanzania

Email: *kbaruku@gmail.com

How to cite this paper: Kasuga, B., Park, E. and Machunda, R.L. (2018) Inhibition of Aluminium Corrosion Using *Carica papaya* Leaves Extract in Sulphuric Acid. *Journal of Minerals and Materials Characterization and Engineering*, 6, 1-14.

<https://doi.org/10.4236/jmmce.2018.61001>

Received: October 20, 2017

Accepted: December 22, 2017

Published: December 25, 2017

Copyright © 2018 by authors and Scientific Research Publishing Inc.

This work is licensed under the Creative Commons Attribution-NonCommercial International License (CC BY-NC 4.0).

<http://creativecommons.org/licenses/by-nc/4.0/>



Open Access

Abstract

Inhibition of aluminium corrosion using *C. papaya* leaves extract in 1.0 M H₂SO₄ was investigated by using gravimetric analysis at various concentrations and temperatures: 303 K, 313 K and 323 K. Characterization was done by using Scanning Electron Microscope (SEM) and Fourier Transform Infrared (FT-IR) spectroscopy. Results show that, inhibiting ability of the extract was due to its adsorption onto the metal surface through Langmuir adsorption isotherm. Thermodynamic (Gibbs energy, entropy and heats of adsorption) and kinetic parameters (activation energy and entropy of activation) were also determined. All of these agreed to physical adsorption of inhibitor onto the aluminium surface.

Keywords

C. papaya, Inhibition, Aluminium, Sulphuric Acid, Adsorption, Thermodynamic and Kinetic Parameters

1. Introduction

Although aluminium is thermodynamically reactive, it is the only metal with a property of protecting itself against corrosion by forming an amphoteric oxide film, which protects it against further attack when found under aggressive medium. In highly aggressive medium, of either alkalinity ($p^H > 9$) or acidity ($p^H < 5$), aluminium and its alloys corrodes by dissolving of its protective oxide layer [1] [2]. Various industrial applications may cause aluminium to come into contact with aggressive media. Some of them include pickling [3], anodizing (surface treatments) [4] and metal cleaning/descaling which involves the

use of H_2SO_4 , HCl , H_3PO_4 and other acids. To overcome such situation corrosion inhibitor are introduced to control and rescue the metal from being attacked.

Interest of investigating plants' extracts as corrosion inhibitors is increasing nowadays due to the fact that, synthetic (inorganic) corrosion inhibitors such as chromates, phosphates, and molybdates have some kind of toxicity. Researches show that plants' extracts are rich in phytochemicals with heteroatoms such as S, O and N which makes them active in developing inhibitive properties [5]. Also it has been reported especially for those with S and N are suitable in acids [6]. Various plants' extracts have been investigated and show good inhibitive ability. *C. papaya* has been reported several times to have a wide spectrum of phytochemicals which among of them are corrosion inhibitive. Some of the reported findings involve, *C. papaya* extracts on the corrosion of mild steel [7], inhibition effect of extracts of *C. papaya* and *Camellia sinensis* leaves [8], electrochemical corrosion behaviour of mild steel reinforced concrete in H_2SO_4 [9], performance of mild steel in nitric acid/*C. papaya* leaf extracts corrosion [10] and synergistic effects of *C. papaya* leaves extract with Zn^{2+} in corrosion inhibition of mild steel in aqueous medium [11]. In the current study *C. papaya* has been investigated as a corrosion inhibitor of aluminium in 1.0 M H_2SO_4 . Gravimetric analysis (Weight loss method) employed in this study is associated with, inhibition efficiency, degree of surface coverage and corrosion rate as follows:

Inhibition efficiency,

$$\% IE = \left(1 - \frac{W_{inh}}{W_{blank}} \right) \times 100 \quad (1)$$

Degree of surface coverage,

$$\theta = 1 - \frac{W_{inh}}{W_{blank}} \quad (2)$$

where, % IE = Inhibition efficiency, W_{inh} = Weight loss in presence of inhibitor, W_{blank} = Weight loss in absence of inhibitor and θ = Surface coverage of inhibitor [12] [13].

The corrosion rate using the formula.

$$CR \left(g \cdot cm^{-2} \cdot h^{-1} \right) = \frac{W}{At} \quad (3)$$

where, CR = Corrosion rate, A = Coupons surface area (cm^2), t = immersion time in hours and W = Weight loss [14] [15].

In case of activation energy values; equation below was used

$$\ln CR = \frac{-E_a}{RT} + \ln A \quad (4)$$

where, $\ln CR$ versus $\frac{1}{T}$ is a straight line with a slope of $-\frac{E_a}{R}$ which is used to calculate the activation energies [14] [16].

Enthalpies of activation values are obtained by plotting the graph of $\ln \frac{CR}{T}$ versus $\frac{1}{T}$, for each temperature. $-\frac{\Delta H_a^0}{R}$ values as slopes were used to calculate the enthalpies of activation and $\ln \left(\frac{R}{Nh} \right) + \frac{\Delta S_a^0}{R}$ as intercepts to calculate entropies. Below is the equation used

$$CR = \frac{RT}{Nh} \exp \left(\frac{\Delta S_a^0}{R} \right) \exp \left(-\frac{\Delta H_a^0}{RT} \right) \quad (5)$$

where h is the plank's constant 6.626176×10^{34} and N is the Avogadro's number, $6.02252 \times 10^{23} \text{ mol}^{-1}$.

ΔS_a^0 is the entropy of activation and ΔH_a^0 is the enthalpy of activation.

Determination of heats of adsorption;

$\ln \left(\frac{\theta}{1-\theta} \right)$ versus $\frac{1}{T}$ is plotted for each concentration and $-\frac{Q_{ads}}{2.303R}$ as the slope is used to calculate the heats of adsorption. Below is the equation used

$$\ln \left(\frac{\theta}{1-\theta} \right) = \log A + \log K - \frac{Q_{ads}}{2.303R} \left(\frac{1}{T} \right) \quad (6)$$

where: θ is a degree of Surface Coverage [14].

Gibbs energy of adsorption is calculated using the formula below

$$\Delta G = -RT(55.5K) \quad (7)$$

where,

$$K = \frac{\theta}{(1-\theta)C}$$

θ = Degree of surface coverage, K = Adsorption equilibrium constant and C = Concentration [17].

In order to study the interaction (mechanism of adsorption) between the metal (aluminium) and inhibitor molecules; various adsorption isotherms have been tested. The adsorption taken place follows the Langmuir adsorption isotherm by having a high correlation coefficient. It obeys the following equation:

$$\frac{C}{\theta} = \frac{1}{K} + C \quad (8)$$

Other isotherms tested and equations used,

Frumkin Isotherm

$$\left(\frac{\theta}{1-\theta} \right) \exp(-2a\theta) = KC \quad (9)$$

Temkin Isotherm

$$\exp(-2a\theta) = KC \quad (10)$$

Freundlich Isotherm

$$\log \theta = \log K + n \log C \quad (11)$$

where C = Concentration, θ = Degree of surface coverage, a = molecular interaction parameter, n = Slope and K = Equilibrium Constant of adsorption [18] [19]

[20].

2. Materials and Methods

2.1. Materials Preparation

2.1.1. Sample Collection

C. papaya leaves used in this investigation were collected from farms of villagers around our campus, Tengeru area, Arumeru District in Arusha, Tanzania. They were air dried for two weeks, then ground by electrical grinder to a fine powder.

2.1.2. Preparation of an Extract

In each of the batch experiments conducted at specific temperatures, three liters (3 L) of 1.0 M H₂SO₄ were firstly prepared and then used to prepare the extract and the corrosive media. Inhibitor (the extract) preparation was done by mixing two liters (2 L) of the acid with 200 g of the *C. papaya* leaves powder into two different one liter (1 L) pyrex conical flasks, in a ratio of 10 g of the leaves powder per 100 mls of the acid. This ratio was taken because on testing various ratios, it was found to be most efficient. The mixture obtained was boiled at 90°C using a heating plate for three hours with a stir (Thermometer was used to maintain such temperature). Then it was left to cool at room temperature for 24 hours and then filtered by firstly using a sieve, centrifuged and finally with Whatman No. 1 filter papers. After filtering, the obtained solution was a corrosion inhibitor (itself with 100 v/v% concentration). From that inhibitor, other concentrations (20, 40, 60, and 80) v/v% were prepared by diluting it with the remained one liter (1 L) of 1.0 M H₂SO₄ at various ratios [13] [21] [22] [23] [24].

2.1.3. Aluminium Coupons Preparation

The coupons with 2 cm × 2 cm × 0.12 cm in dimensions were filed by using emery papers (# 400, 600, 800, 1000, and 1200), washed with ethanol, dried with acetone, and then stored in desiccators until used. Elemental composition of aluminium used to prepare the coupons (Table 1) was determined using a Wavelength-dispersive X-ray fluorescence Spectroscopy (WDXS).

2.2. Gravimetric Analysis (Weight Loss Measurements)

In this method a Denver analytical balance with an accuracy of 0.0001 g was used. Coupons' weights were measured before and after they have been immersed in the corrosive media. Distilled water, ethanol, acetone and desiccators were used to wash and dry the coupons several times before taking measurements. In every batch experiment, each coupon was immersed for 24 hours in a 150 ml beaker. The total volume of the medium in each beaker was made up to 100 ml. The experiments were done at concentrations of a blank, (20, 40, 60, 80 and 100) v/v% and temperatures of 303 K, 313 K and 323 K. All beakers were put in water baths to control such temperatures. The experiments were repeated three times and the average weights lost were recorded and then well analysed.

Table 1. Elemental composition of aluminium (%).

Element	%	Element	%
Al	98.94	Cu	0.004
Mg	0.35	Cr	0.0029
Si	0.34	P	0.002
Fe	0.26	Mn	0.0017
Ti	0.0097	Ag	0.0004
Ni	0.0008	Pb	0.0004
V	0.0069	Co	0.0003
Zn	0.004		

Table 2. Shows the average weight loss and calculated corrosion rate for each experiment.

Conc. (v/v%)	Weight loss (g) and Inhibition efficiency						CR (gcm ⁻² h ⁻¹) (10 ⁻⁵)		
	303 K	I.E%	313 K	I.E%	323 K	I.E%	303 K	313 K	323K
Blank	0.012		0.0359		0.0856		5.580	16.695	39.807
20	0.0049	59.17	0.015	58.32	0.0428	50.00	2.279	6.975	19.903
40	0.0038	68.33	0.013	63.88	0.0378	55.84	1.767	6.045	17.578
60	0.0034	71.67	0.0122	65.98	0.0354	58.64	1.581	5.673	16.462
80	0.0034	71.67	0.0118	67	0.036	57.94	1.581	5.487	16.741
100	0.0036	70.00	0.0126	65.9	0.0384	55.14	1.674	5.859	17.857

2.3. Surface Characterization

Surface morphology was examined using a Field Scanning Electron Microscope (FE-SEM, Hilachi, S-4700). BRUKER FTIR spectrometer in transmittance mode with a spectral range of 4000 - 500 cm⁻¹ was used to ascertain functional groups of the extract associated with corrosion inhibition action.

3. Results and Discussion

3.1. Weight Loss, Inhibition Efficiency and Corrosion Rate Values

Table 2 and **Figure 1** show that: Inhibition efficiency increases with increasing in concentration and decreases with the rise in temperature. The maximum inhibition efficiency at 303 K, 313 K and 323 K is 71.67%, 67% and 58.64% respectively. Concentration at which maximum adsorption has taken place (optimal concentration) of inhibitor at 303 K, 313 K and 323 K is 60%, 80% and 60% v/v respectively.

3.2. Kinetic and Thermodynamic Parameters

Kinetic and thermodynamic parameters include: activation energy— E_a (J/mol), enthalpy of activation— $+\Delta H$ (kJ/mol), entropy of adsorption— ΔS^0 (J/mol), heat energy of adsorption— ΔQ_{ads} (kJ/mol) and Gibbs energy of adsorption— ΔG^0 (J/mol) were determined and recorded in **Table 3**. Determination of activation energy was done by plotting the graphs of \ln (Corrosion rate) vs $1/\text{Temperature}$ using Equation (4). Their slopes $-\frac{E_a}{R}$ obtained were then used

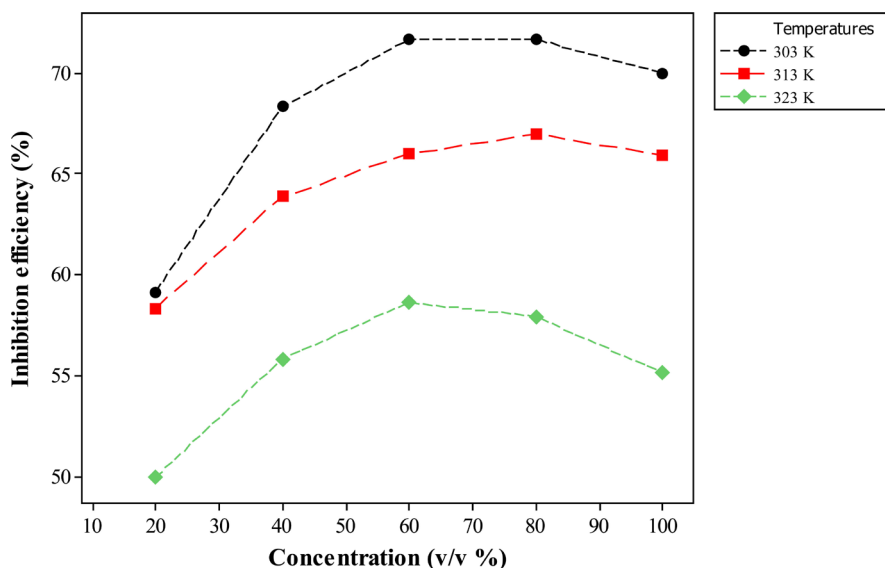


Figure 1. The relationship between inhibition efficiency and concentration at various temperatures.

Table 3. Shows kinetic and thermodynamic parameters.

Conc. v/v%	E_a kJ/mol	$+\Delta H$ kJ/mol	ΔS° J/mol	ΔQ_{ads} (kJ/mol)	ΔG (kJ/mol)		
					303 K	313 K	323 K
Blank	80.01	77.40	-70.75				
20	88.18	85.58	-51.46	14.96	-3.51	-3.53	-2.74
40	93.50	86.42	-35.92	21.67	-2.76	-2.34	-1.51
60	95.38	92.78	-30.59	23.51	-2.14	-1.52	-0.73
80	96.03	93.42	-28.52	24.64	-1.42	-0.89	0.12
100	96.33	93.73	-27.02	26.00	-0.65	-0.18	1.03

in calculations (**Figure 2** indicates the summary graph at various concentrations of the inhibitor).

Enthalpy of activation and entropy of adsorption were determined by plotting graphs of $\ln(\text{Corrosion rate}/\text{Temperature})$ vs $1/\text{Temperature}$ using Equation (5), then $-\frac{\Delta H^0}{R}$, as slopes to calculate the enthalpy of activation and $\ln\left(\frac{R}{Nh}\right) + \frac{\Delta S^0}{R}$ as intercepts to calculate the entropy of adsorption (**Figure 3** is the summary graph at various concentrations).

Heats of adsorption were determined by plotting graphs of $\text{Log} [\text{Surface coverage}/(1-\text{Surface Coverage})]$ using Equation (6), and $-\frac{Q_{ads}}{2.303R}$, as slopes were used in calculations (**Figure 4** is the summary graph at all concentrations of inhibitor 0%, 20%, 40%, 60%, 80% and 100%). Gibbs energy of adsorption was determined using Equation (7).

The increase in activation energy of the metal dissolution was due to the increase in the inhibitor concentration and its adsorption. This is because the in-

hibitor adsorption on the metal surface hindered the metal dissolution [25] [26]. The positive values of enthalpy of activation show the endothermic nature of the metal dissolution which is associated with the rise in corrosion rate of the metal at high temperatures [6].

Increasing in entropy (from most negative to less negative values), shows the increase in disorder at the metal and solution interface which is due to the desorption of water molecules from the surface of the metal by molecules of the inhibitor [6]. The increase in the heats of adsorption with the increase in concentration of the inhibitor, shows the exothermic nature of its adsorption [25]. Gibbs energy increased (from most negative to less negative) as the temperature rises also implies the exothermic nature of the adsorption process [14]. This means that at high temperature there was desorption of the inhibitor on the metal surface. Adsorption isotherms together with the kinetic and thermodynamic parameters helped to determine whether the adsorption process was

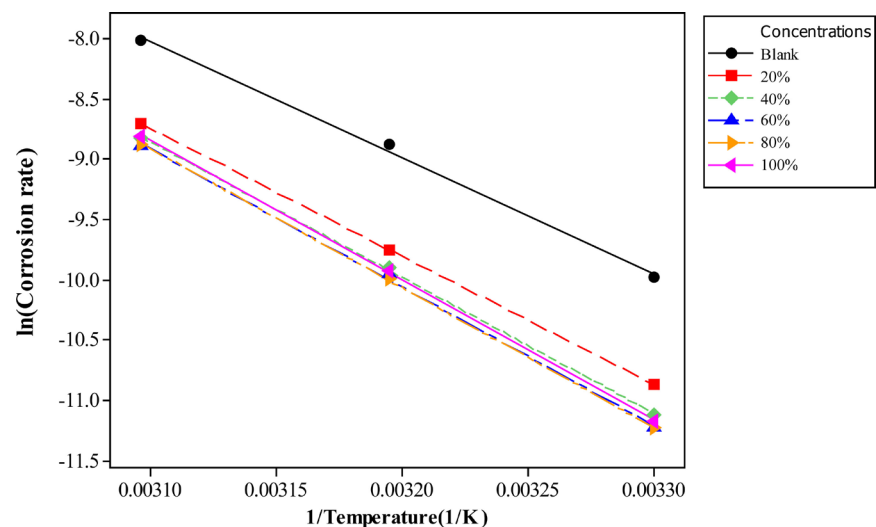


Figure 2. A plot of $\ln(\text{Corrosion rate})$ vs $1/\text{Temperature}$.

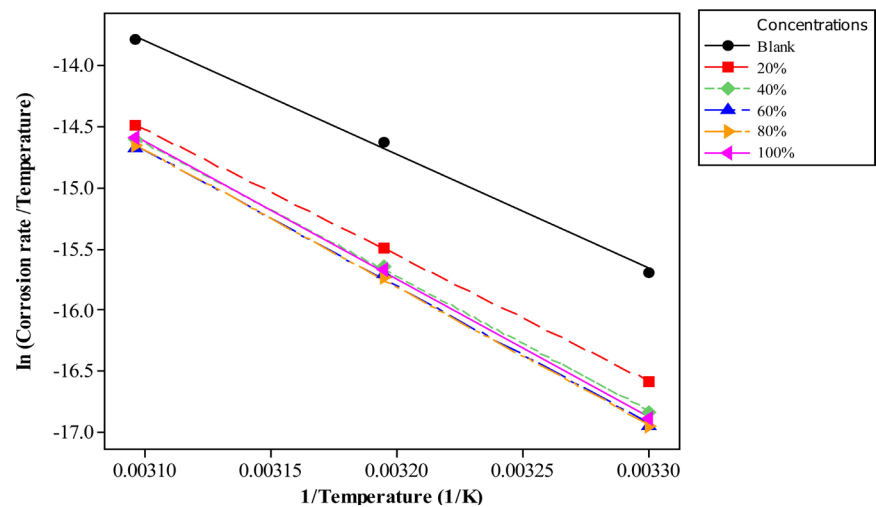


Figure 3. A plot of $\ln(\text{Corrosion rate}/\text{Temperature})$ vs $1/\text{Temperature}$.

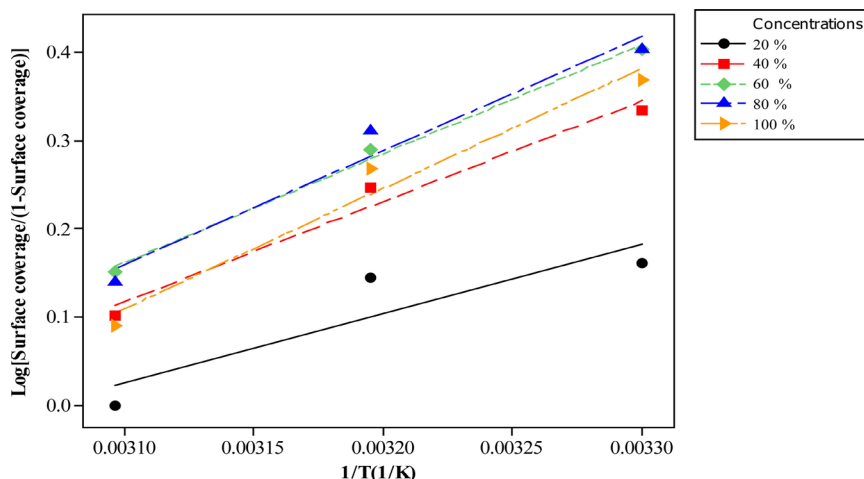


Figure 4. A plot of $\text{Log} [\text{Surface coverage}/(1-\text{Surface Coverage})]$.

Table 4. A summary of correlation coefficients for the Isotherms tested.

Isotherm	Correlation coefficient value (R^2) at various temperatures		
	303 K	313 K	323 K
Frumkin	0.561	0.794	0.383
Freundlich	0.786	0.869	0.565
Temkin	0.787	0.873	0.553
Langmuir	0.997	0.998	0.995

achieved through physical or chemical mechanism. In the current study all parameters agreed to physical adsorption of the inhibitor on the metal surface.

3.3. Adsorption Isotherms

Since the inhibitor works through adsorption onto the metal surface, various adsorption isotherms were tested includes: Frumkin, Freundlich, Temkin and Langmuir adsorption isotherms using Equations (8)-(11) respectively. **Table 4** shows correlation coefficient values for each isotherm at various temperatures as have been tested.

The adsorption of the inhibitor onto the metal surface seems to obey Langmuir adsorption isotherm by having a high correlation coefficient of approximately equal to 1. This isotherm goes with assumption that, there is no lateral interaction between the adsorbed species and the adsorbent. **Figure 5** shows the Langmuir adsorption isotherm plot.

3.4. FT-IR Spectroscopy Analysis

FT-IR test was performed to the *C. papaya* leaves powder, inhibitor prepared by using 1.0 M H_2SO_4 and the corrosion product (adsorbed film). In case of the leaves powder a little amount of the sample was tested and in corrosion inhibitor few drops were tested. A test concerning a corrosion product was done by firstly preparing the aluminium coupon. The coupon was prepared by being abraded

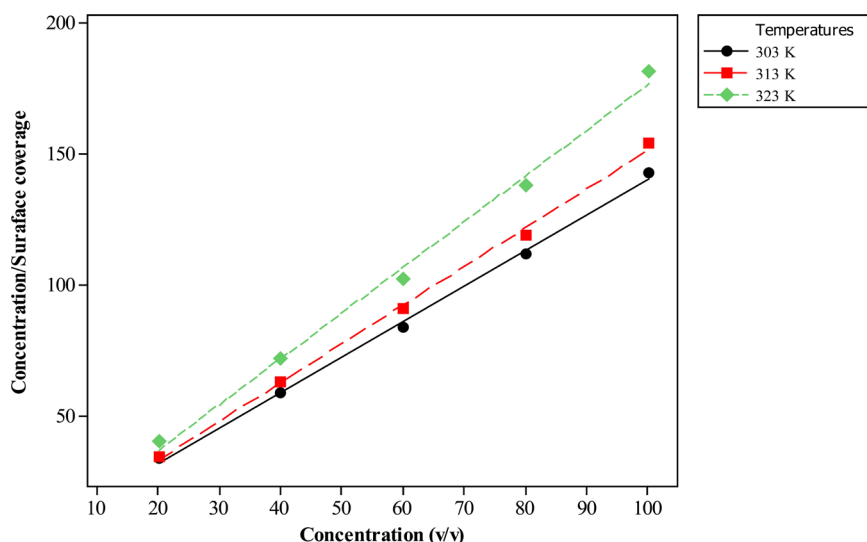


Figure 5. Langmuir adsorption isotherm plot at various temperatures.

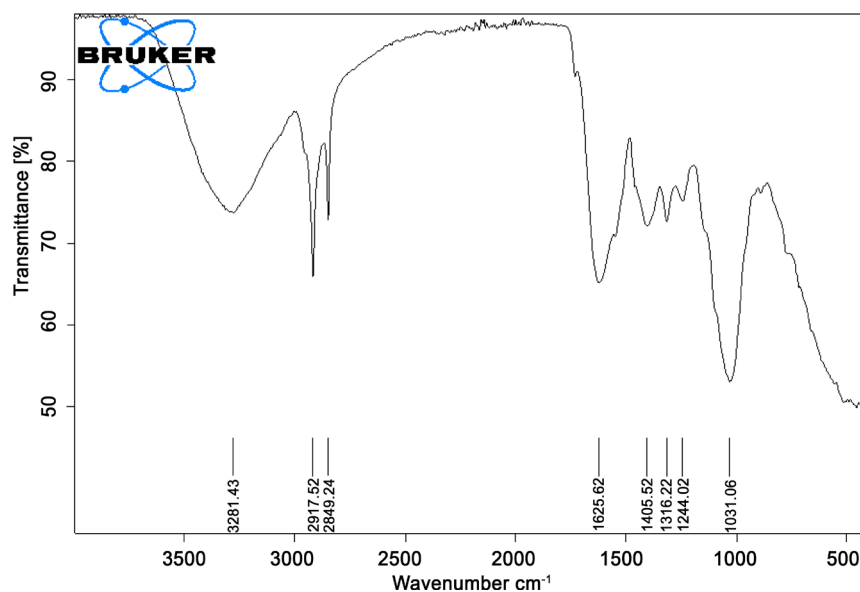


Figure 6. *C. papaya* leaves powder.

with emery papers, then washed with ethanol and dried with acetone. The prepared coupon was immersed in 60 v/v% inhibitor (optimal concentration) in 100 mls of the medium (150 mls beaker was used), for 24 hrs at 30°C. Then after, a coupon was scrapped to get a corrosion product which was FT-IR tested. The results obtained here were the FT-IR spectra of the *C. papaya* leaves, inhibitor and the corrosion product shown in Figures 6-8 respectively.

Table 5 shows functional groups identified from *C. papaya* leaves powder, inhibitor prepared by using H_2SO_4 and the corrosion product (adsorbed film) using FT-IR spectroscopy. Absorption frequencies in the table are the values recorded from the FT-IR spectra (Figures 6-8). The functional groups assigned from *C. papaya* leaves, prepared inhibitor and adsorbed film, are those functional groups found to participate in the adsorption and inhibition of various

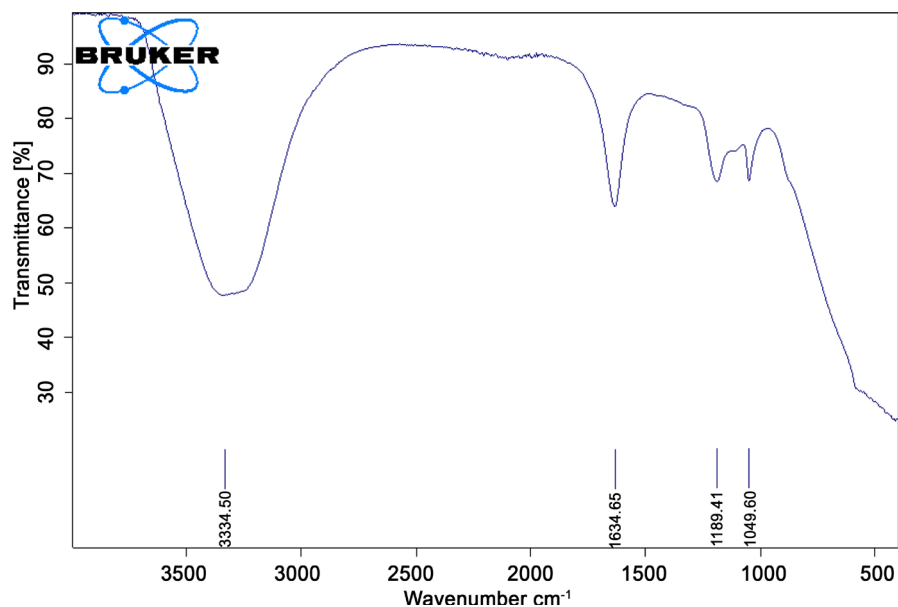


Figure 7. Inhibitor prepared using H_2SO_4 .

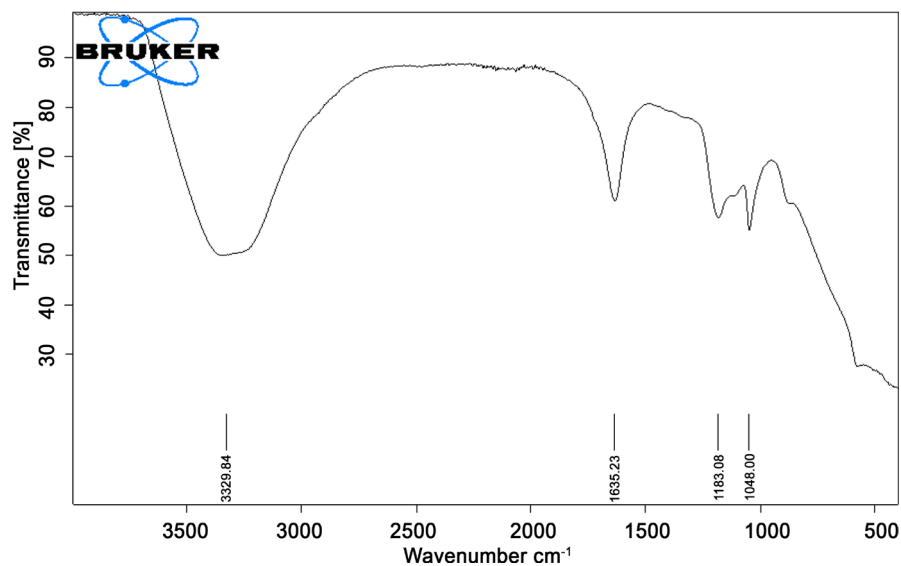


Figure 8. Adsorbed film formed after using H_2SO_4 .

inhibitors which have been reported. The shift of these frequencies from inhibitor to the adsorbed ones can be attributed to the interaction of inhibitor functional groups with the metal surface for the adsorption to take place.

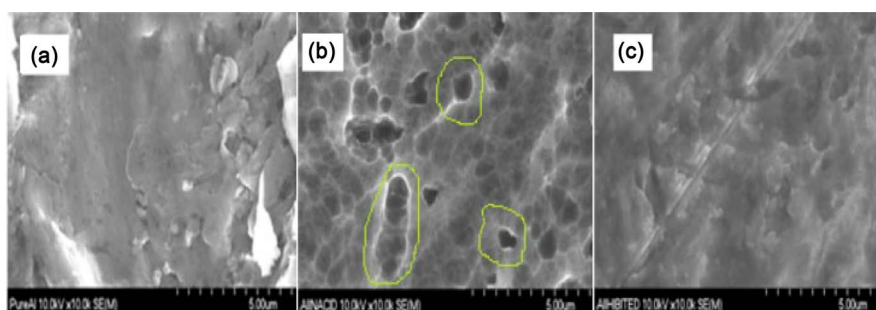
For example O-H vibration shifted from 3334.5 cm^{-1} to 3329.84 cm^{-1} and that of C=O from 1634.65 cm^{-1} to 1635.23 cm^{-1} [22] [27] [28].

3.5. Surface Profile Analysis Using SEM

Uncorroded, uninhibited and inhibited coupons were examined by using Scanning Electron Microscope (SEM). Uninhibited and inhibited coupons were dipped in the medium (100 ml of 1.0 M H_2SO_4) for 24 hours at 30°C before analysis. For inhibited coupon, inhibitor was added at the optimal concentration of 60 v/v%.

Table 5. FT-IR spectroscopy results (H_2SO_4 medium).

Leaves powder		Inhibitor prepared using H_2SO_4		Corrosion product	
Frequency (cm^{-1})	Assignment	Frequency (cm^{-1})	Assignment	Frequency (cm^{-1})	Assignment
3281.43	-OH or N-H Stretch	3334.5	O-H Stretch	3329.84	O-H Stretch
2917.52	-C-H Stretch	1634.65	C=O Stretch	1635.23	C=O Stretch
2849.24		1189.41	C-O or C-H Stretch	1183.08	C-O or C-N Stretch
1625.62	C=O stretch	1049.60		1048.00	
1405.52	C-H bending				
1316.22					
1244.02	C-O or C-N stretch				
1031.06					

**Figure 9.** SEM images of aluminium at various conditions.

From **Figure 9** above coupons with different treatment displayed different images from SEM; (a) Uncorroded surface of aluminium coupon without pits, but some scratches which occurred during filing (b) Uninhibited coupon with deep pits (some of them are overlaid by the lines in order to become easily seen) shows corrosion has taken place (c) Inhibited coupon which shows the protected surface which is not much affected by the acid. From the surface profile of aluminium coupons done, the difference indicated above, proves the formation of the adsorbed layer (film) which acted as a barrier to the acid corrosiveness [17] [29].

4. Conclusions

1) *C. papaya* extracts investigated was found to be among of effective green corrosion inhibitors to the aluminium corrosion under acidic medium. Its action through physisorption of the extract phytochemicals created a corrosion barrier at the metal (aluminium)-solution (acid) interface.

2) The difference in kinetic and thermodynamic parameters in the absence and presence of the extract proved its adsorption.

3) Adsorption isotherms test as a mean to understand the model of adsorption agreed to Langmuir adsorption isotherm.

4) The difference in SEM images of the aluminium surface by the one with inhibitor to be smoother than the surface of without it is also a proof of the inhibitor adsorption as well as its activeness.

Acknowledgements

This work was supported by the Government of Tanzania through Nelson Mandela African Institution of Science and Technology.

References

- [1] Oguzie, E.E. (2007) Corrosion Inhibition of Aluminium in Acidic and Alkaline Media by *Sansevieria trifasciata* Extract. *Corrosion Science*, **49**, 1527-1539. <https://doi.org/10.1016/j.corsci.2006.08.009>
- [2] Li, X. and Deng, S. (2012) Inhibition Effect of *Dendrocalamus brandisii* Leaves Extract on Aluminum in HCl, H₃PO₄ Solutions. *Corrosion Science*, **65**, 299-308. <https://doi.org/10.1016/j.corsci.2012.08.033>
- [3] Zaferani, S.H., *et al.* (2013) Application of Eco-Friendly Products as Corrosion Inhibitors for Metals in Acid Pickling Processes—A Review. *Journal of Environmental Chemical Engineering*, **1**, 652-657. <https://doi.org/10.1016/j.jece.2013.09.019>
- [4] Moutarlier, V., *et al.* (2005) EIS Characterisation of Anodic Films Formed on 2024 Aluminium Alloy, in Sulphuric Acid Containing Molybdate or Permanganate Species. *Corrosion Science*, **47**, 937-951. <https://doi.org/10.1016/j.corsci.2004.06.019>
- [5] Rani, B. and Basu, B.B.J. (2011) Green Inhibitors for Corrosion Protection of Metals and Alloys: An Overview. *International Journal of Corrosion*, **2012**.
- [6] Quraishi, M., *et al.* (2010) Green Approach to Corrosion Inhibition of Mild Steel in Hydrochloric Acid and Sulphuric Acid Solutions by the Extract of *Murraya koenigii* Leaves. *Materials Chemistry and Physics*, **122**, 114-122. <https://doi.org/10.1016/j.matchemphys.2010.02.066>
- [7] Okafor, P. and Ebenso, E. (2007) Inhibitive Action of *Carica papaya* Extracts on the Corrosion of Mild Steel in Acidic Media and Their Adsorption Characteristics. *Pigment & Resin Technology*, **36**, 134-140. <https://doi.org/10.1108/03699420710748992>
- [8] Loto, C., Loto, R. and Popoola, A. (2011) Inhibition Effect of Extracts of *Carica papaya* and *Camellia sinensis* Leaves on the Corrosion of Duplex (α β) Brass in 1M Nitric acid. *International Journal of Electrochemical Science*, **6**, 4900-4914.
- [9] Loto, C. (2012) Electrode Potential Evaluation of Effect of Inhibitors on the Electrochemical Corrosion Behaviour of Mild Steel Reinforcement in Concrete in H₂SO₄. *Journal of Materials and Environmental Science*, **3**, 195-205.
- [10] Oki, M., Anawe, P.A. and Fasakin, J. (2015) Performance of Mild Steel in Nitric Acid/Carica Papaya Leaf Extracts Corrosion System. *Asian Journal of Applied Sciences*, **3**.
- [11] Kavitha, N., Manjula, P. and Anandha, M. (2014) Syneristic Effect of *C. papaya* Leaves Extract-Zn⁺² in Corrosion Inhibition of Mild Steel in Aqueous Medium. *Research Journal of Chemical Sciences*, **4**, 88-93.
- [12] Umoren, S., Ebenso, E. and Ogbobe, O. (2009) Synergistic Effect of Halide Ions and Polyethylene Glycol on the Corrosion Inhibition of Aluminium in Alkaline Medium. *Journal of Applied Polymer Science*, **113**, 3533-3543. <https://doi.org/10.1002/app.30258>

- [13] Nwosu, O., et al. (2014) Acidic Corrosion Inhibition of *Piper guineense* Seed Extract on Al Alloy. *American Journal of Materials Science*, **4**, 178-183.
- [14] Obi-Egbedi, N., Obot, I. and Umoren, S. (2012) *Spondias mombin* L. as a Green Corrosion Inhibitor for Aluminium in Sulphuric Acid: Correlation between Inhibitive Effect and Electronic Properties of Extracts Major Constituents Using Density Functional Theory. *Arabian Journal of Chemistry*, **5**, 361-373.
<https://doi.org/10.1016/j.arabjc.2010.09.002>
- [15] Eddy, N.O., Momoh-Yahaya, H. and Oguzie, E.E. (2015) Theoretical and Experimental Studies on the Corrosion Inhibition Potentials of Some Purines for Aluminum in 0.1 M HCl. *Journal of Advanced Research*, **6**, 203-217.
<https://doi.org/10.1016/j.jare.2014.01.004>
- [16] Nahlé, A., Abu-Abdoun, I.I. and Abdel-Rahman, I. (2012) Effect of Temperature on the Corrosion Inhibition of Trans-4-hydroxy-4'-stilbazole on Mild Steel in HCl Solution. *International Journal of Corrosion*, **2012**, Article ID: 380329.
- [17] Kini, A.U., et al. (2011) Corrosion Inhibition of Al6061-SiC-p Composite in 0.5 M Hydrochloric Acid. *Proceedings of International Conference on Chemistry and Chemical Process*.
- [18] Lebrini, M., Robert, F. and Roos, C. (2013) Adsorption Properties and Inhibition of C38 Steel Corrosion in Hydrochloric Solution by Some Indole Derivates: Temperature Effect, Activation Energies, and Thermodynamics of Adsorption. *International Journal of Corrosion*, **2013**, Article ID: 139798.
- [19] Arockiasamy, P., et al. (2014) Evaluation of Corrosion Inhibition of Mild Steel in 1 M Hydrochloric Acid Solution by *Mollugo cerviana*. *International Journal of Corrosion*, **2014**, Article ID: 679192.
- [20] Fouda, A., et al. (2012) Corrosion Inhibition of Aluminum in $1\text{MH}_3\text{PO}_4$ Solutions by Ethanolamines. *Arabian Journal of Chemistry*, **5**, 297-307.
<https://doi.org/10.1016/j.arabjc.2010.08.020>
- [21] Avwiri, G.O. and Igho, F. (2003) Inhibitive Action of *Vernonia amygdalina* on the Corrosion of Aluminium Alloys in Acidic Media. *Materials Letters*, **57**, 3705-3711.
[https://doi.org/10.1016/S0167-577X\(03\)00167-8](https://doi.org/10.1016/S0167-577X(03)00167-8)
- [22] Leelavathi, S. and Rajalakshmi, R. (2013) *Dodonaea viscosa* (L.) Leaves Extract as Acid Corrosion Inhibitor for Mild Steel—A Green Approach. *Journal of Materials and Environmental Science*, **4**, 625-638.
- [23] Prabhu, D. (2013) Studies of Corrosion of Aluminium and 6063 Aluminium Alloy in Phosphoric Acid Medium. *International Journal of ChemTech Research*, **5**, 2690-2705.
- [24] Loto, C., et al. (2014) Corrosion Inhibitive Behaviour of *Camellia Sinensis* on Aluminium Alloy in H_2SO_4 . *International Journal of Electrochemical Science*, **9**, 1221-1231.
- [25] Obot, I., Umoren, S. and Obi-Egbedi, N. (2011) Corrosion Inhibition and Adsorption Behaviour for Aluminium by Extract of *Aningeria robusta* in HCl Solution: Synergistic Effect of Iodide Ions. *Journal of Materials and Environmental Science*, **2**, 60-71.
- [26] Hamdy, A. and El-Gendy, N.S. (2013) Thermodynamic, Adsorption and Electrochemical Studies for Corrosion Inhibition of Carbon Steel by Henna Extract in Acid Medium. *Egyptian Journal of Petroleum*, **22**, 17-25.
<https://doi.org/10.1016/j.ejpe.2012.06.002>
- [27] Sangeetha, M., et al. (2012) Eco-Friendly Extract of Banana Peel as Corrosion Inhibitor for Carbon Steel in Sea Water. *Journal of Natural Product and Plant Re-*

sources, **2**, 601-610.

- [28] Eddy, N.O. (2009) Inhibitive and Adsorption Properties of Ethanol Extract of *Colocasia esculenta* Leaves for the Corrosion of Mild Steel in H₂SO₄. *International Journal of Physical Sciences*, **4**, 165-171.
- [29] Arellanes-Lozada, P., *et al.* (2014) The Inhibition of Aluminum Corrosion in Sulfuric Acid by Poly (1-vinyl-3-alkyl-imidazolium hexafluorophosphate). *Materials*, **7**, 5711-5734. <https://doi.org/10.3390/ma7085711>